Characterization of Particle-Interactions by Atomic Force Microscopy: Effect of Contact Area

Jennifer C. Hooton,[1] Caroline S. German,[2] Stephanie Allen,[1] Martyn C. Davies,[1] Clive J. Roberts,[1,3] Saul J. B. Tendler,[1] and Philip M. Williams[1]

Received October 30, 2002; accepted December 4, 2002

Purpose. The purpose of this work was to compare adhesion forces, contact area, and work of adhesion of salbutamol sulphate particles produced using micronization and a supercritical fluid technique (solution-enhanced dispersion by supercritical fluids – SEDS™) using atomic force microscopy (AFM).

Methods. Adhesion forces of individual particles of micronized and SEDS™ salbutamol against a highly orientated pyrolytic graphite surface were acquired in a liquid environment consistent with that of a pressurized metered dose inhaler. The forces were then related to contact area and work of adhesion.

Results. The raw adhesion force data for the micronized and SEDS™ material were 14.1 nN (SD 2.5 nN) and 4.2 nN (SD 0.8 nN), respectively. After correction for contact area, the forces per unit area were 13 mN/μm^2 (SD 2.3 mN/μm^2) and 3 mN/μm^2 (SD 0.6 mN/μm^2). The average work of adhesion was calculated using the Johnson-Kendall-Roberts theory and was found to be 19 mJm^{-2} (SD 3.4 mJm^{-2}) for the micronized particle and 4 mJm^{-2} (SD 0.8 mJm^{-2}) for the SEDS™ particle.

Conclusions. It is possible to produce a three-dimensional representation of the contact area involved in the interaction and make quantitative comparisons between different particles. There was a lower force per unit area and work of adhesion observed for the SEDS™ material, possibly because of its lower surface free energy.

KEY WORDS: SEDS; micronized; AFM; contact area; work of adhesion.

INTRODUCTION

The ability to produce free-flowing particles with controlled particle size, size distribution, and morphology is a requirement of many aspects of pharmaceutical production, for example, in processes requiring powder flow such as tablet manufacture. Although current methods are generally able to achieve these aims, they are often limited in that the particles can be cohesive with minimal scope for the improved control of their physical characteristics.

Numerous methods have been used to investigate the adhesive properties of particles, for example centrifuge techniques (1). A recent addition to these approaches has been the atomic force microscope (AFM; Ref. 2). The ability to measure forces between individual particles adhered to AFM tips and a surface was demonstrated soon after the AFM was invented (3). It has since been used to examine the forces between many different systems and environments (4,5). The AFM has also been used to acquire force measurements relevant to pharmaceuticals applications (6,7).

There are a number of factors that are important in particle adhesion, including capillary, electrostatic and van der Waals forces, and the surface free energy of the particle. In this work, van der Waals forces and surface energy are of most relevance. This is because capillary forces are eliminated in a liquid environment, and electrostatic forces have been found unlikely to play a part in the interaction (8). Some discussions of the potential role of cavitation forces in such interactions have been reported (9); however, this possibility remains to be investigated within our studies and is outside the framework of the theoretical model used in this work. For van der Waals forces, an increase in the contact area will lead to an increase in the area over which such short range forces can act. For surface free energy, this can be calculated for a unit area of a solid, through its relationship to the work that must be done to separate two surfaces by the equation,

$$W = \gamma^a + \gamma^b - \gamma^{ab} \quad (1)$$

Where W is work of adhesion (mJm^{-2}), γ^a and γ^b (mJm^{-2}) are the free energies per unit surface area of solids a and b, and γ^{ab} is the free energy of the a–b interface (10). Clearly, knowledge of the contact area is important in understanding the adhesion.

A frequent limitation of AFM-based force measurements of individual particulate interactions is that it has not been possible to estimate the area of interaction, limiting the ability to undertake quantitative comparisons of forces between different particles. In this article, a method first suggested by Neto and Craig (11) using tip characterization gratings to characterize colloidal probe particles has been extended to estimate the contact area of pharmaceutical particles involved in AFM force distance measurements. We have used this knowledge to examine the differences in adhesion observed between particles of the same material produced using different manufacturing techniques.

A novel approach for particle production has been the use of supercritical fluids (12). A supercritical fluid (SCF) is a substance at a temperature and pressure above its critical point, and such SCFs have been successfully used in pharmaceutical particle production as solvents (13,14). However, because of the limited solubility of many drugs in SCFs, the most commonly used approach has been that of the antisolvent (15,16). This has been developed in a number of ways to produce particles. One such method is the solution enhanced dispersion by supercritical fluids (SEDS™) technique (17). This uses a specially designed nozzle in which flow rates, pressure, and temperature conditions are regulated to allow the control over particle properties. SEDS™ has been shown to produce micrometre particles of narrow size distribution, which are free flowing (12,18,19). The enhanced flow properties are thought to be caused by the particles having a relatively smooth surface morphology and low surface energy compared with particles made with established methods, such as micronization.

[1] Laboratory of Biophysics and Surface Analysis, School of Pharmaceutical Sciences, University of Nottingham, NG7 2RD, United Kingdom.

[2] Bradford Particle Design Ltd, 69 Listerhills Science Park, Campus Road, Bradford, BD7 1HR, United Kingdom.

[3] To whom correspondence should be addressed. (e-mail: clive.roberts@nottingham.ac.uk)

0724-8741/03/0300-0508/0 © 2003 Plenum Publishing Corporation

In this study, particles of salbutamol sulphate produced using both the SEDS™ technique and micronization were mounted onto AFM probes, and force data were acquired in a liquid environment. Operation in a liquid removes the effect of capillary forces between particles. The liquid chosen was 2H 3H perfluropentane because it has industrial applications in a model propellant system for the simulation of environments in pressurized inhaler systems (20). The contact area involved in the interaction was then assessed and related to the force measurements. From this, a quantitative comparison in terms of force of interaction per unit area and work of adhesion was made between micronized and SEDS™ salbutamol.

MATERIALS AND METHODS

Particle Placement on AFM Tips

Silicon nitride v-shaped cantilevers were plasma etched with oxygen at 10W for 30 s (RF plasma barrel etcher PT7100, Bio-Rad, Hercules, CA, USA). The spring constant was then determined using the thermal method (21). Particles of SEDS™ salbutamol (bpd sample no 0141025) and micronized salbutamol (bpd sample no 020/99-03) were then mounted onto the cantilever apex using a Nanoscope IIIa MultiMode AFM (Digital Instruments, Santa Barbara, CA, USA). A clean metal stub was prepared with glue (Loctite, Hertfordshire, UK) on one half and particles of salbutamol on the other. An old tip was then used to draw out a thin line of glue on the substrate. This tip was then replaced with the plasma-etched tip to which the particle was to be added. The tip was first placed over the glue and then brought into contact. The tip was then repositioned over an individual particle before being brought into contact with it. The tip was then retracted and left for 24 h to allow the glue to dry.

To check that particles had been successfully added onto the cantilevers, the tips were examined by scanning electron microscopy (SEM; SEM 505, Philips Amsterdam, Holland). The tips were mounted onto metal stubs using carbon tape but were not gold coated before imaging using an accelerating voltage of approximately 12 kV.

Force–Distance Measurements

The essential part of an AFM is the cantilever with a tip integrated on the underside. A laser beam is deflected off the cantilever onto a quadrant photodiode detector, which is connected via a feedback loop to the piezo upon which either the sample or tip is positioned. In constant force mode the force between the tip and the sample is maintained at a constant level so that any changes in the surface topography cause changes in cantilever deflection, which are detected via the photodiode signal. This leads to an adjustment in the height of the piezo to compensate for this deflection so that the force is maintained. The ability of the cantilever to detect interactions between the tip and the substrate allows it to be used not only for topography imaging but also force distance measurements. A Topometrix Explorer AFM (ThermoMicroscopes, CA, USA) was used to obtain both force and image data. The prepared tips were mounted onto half moon metal stubs using epoxy adhesive (Araldite Bostik, Findley, Stafford, UK) and allowed to dry overnight. These were then placed on a liquid scanner with a Z range of 12 μm (ThermoMicroscopes). The scanner was then lowered into a sample chamber containing approximately 5 mL of 2H 3H perfluropentane (Apollo Scientific Limited, Derbyshire, UK).

The substrate against which force distance measurements were undertaken was freshly cleaved highly orientated pyrolytic graphite (HOPG; Agar Scientific, Essex, UK), which was adhered to the base of the sample chamber. The surface roughness (Rq) was determined to be 0.207 nm using contact mode AFM imaging and a scale of 1 μm^2. This low level of roughness, combined with the inertness of HOPG, means that performing measurements against different areas of the substrate would not unduly affect measurements taken using different tips.

For each of the tips, approximately 70 force measurements were obtained. A typical force curve is shown in Fig. 1. Initially, the probe is a distance away from the surface of the sample (a), and the cantilever deflection is at its rest position known as the free level. The probe is then moved toward the sample surface until they come into contact (b). Once in contact with the surface, any further movement of the probe toward the sample will cause the tip to indent into the surface or the supporting cantilever to bend further. When a predefined point (the set point, c) is reached, the tip is retracted way from the surface. If adhesion occurs between the probe and the sample surface the retract trace will not follow the approach trace, and a trough is observed to occur (d). When the movement of the probe away from the surface is sufficient to overcome the adhesion, the probe leaves the surface to return to the original starting level (a). By measuring the distance *d,* between the trough (d) and the free level (a), it is possible to calculate the adhesion force using Hookes law,

$$F = -kd \tag{2}$$

where F is the force of adhesion (nN) and k is the spring constant of the cantilever (nN/nm). For each measurement the same set points and free levels were used. All data were processed using custom-written force curve analysis software. These results were then used to produce log-normal plots of the adhesion forces recorded in these experiments.

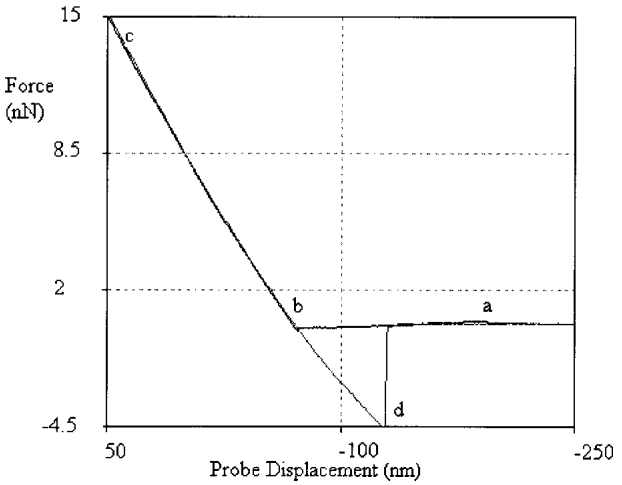

Fig. 1. A typical force distance curve obtained for a single measurement of a particle against a highly orientated pyrolytic graphite surface.

To confirm that it was the particles and not the tips coming into contact with the surface, two control experiments were undertaken. These consisted of force distance measurements with a plasma etched tip and a plasma etched tip that had been dipped in glue but had no subsequent addition of a particle.

Determination of the Profile of Particles on AFM Tips

The particle tips were imaged using a tip characterization grating (TGT01, NT-MDT, Moscow, Russia) which consists of an array of inverted sharp tips. As the cantilevers were scanned across the grid, the particles on the tips were imaged due to an artefact of AFM known as tip imaging (22,23), which occurs when the dimensions of features on a sample surface are of the same order or sharper than that of the imaging probe. When a probe is passed over such a surface changes in cantilever deflection are due to the surface features of the probe and not the sample surface. This effectively creates an image of the probe and not the sample surface. The image produced is a convolution of the features of the tip and the sample. However, because the cone angle of the characterizer tip is 20°, compared to 70° for the contact tips used in this study, this effect was not considered to be critical.

A 10-μm image was acquired of each tip using a scan rate of approximately 0.5 μm/s. To show that the particles were being imaged, further imaging work was undertaken using a plasma etched cantilever with no particle added as a control. This was then scanned across the grid and the image examined to observe for any similarities between this and particles imaged.

After imaging of the tips, they were then re-examined under the SEM to ensure that the particles were still present and had not been removed by imaging, and that no changes in the structure of the particle had occurred.

Image Analysis

Images were analyzed using SPIP software (Image Metrology ApS, Lyngby, Denmark). The images were first passed though a median filter. Because the tip characterization grating caused the particle to be imaged repeatedly, three such repeats of the particle were chosen, and cross sections of each were obtained in both the orthogonal X and Y directions. From these, the radius of a sphere that would fit these cross sections was calculated for both the X and Y direction. Small changes were seen in the cross-sectional data for each of the three repeats taken from the images. Such variations may have been the result of environmental noise but also possibly because of variation in the sharp features of the imaging grid causing small changes in the surface area. The average fitted sphere was then used to calculate the work and force per unit area.

Area and Work of Adhesion Calculations

When a particle comes into contact with a surface, deformation will occur, leading to changes in the contact area. If the Young's modulus of the particle (E_1) is greater than that of the surface (E_2), then the particle will deform the surface, although some particle deformation may also occur, meaning that a common radius of curvature that is a mix of both the surface and particle deformation will result (24,25). Contact mode imaging of the HOPG surface was undertaken before and after force measurements were undertaken with both a blank tip and a tip with a particle added. No changes were seen in the surface structure following the measurements showing that the HOPG was deforming elastically and hence leaving no indent. Because of this, the contact radius of the particle was taken as the common radius of curvature, and was used to calculate contact radius a_0, with the following equation (26):

$$a_0^3 = \frac{3RF_{on}}{4E^*} \tag{3}$$

where R is the radius of the particle, F_{on} is the peak contact force (c, Fig. 1) and E^* is the reduced Young's modulus that occurs at the contact point. To calculate the value of E^*, the following equation was used:

$$\frac{1}{E^*} = \frac{1-\nu_1^2}{E_1} + \frac{1-\nu_2^2}{E_2} \tag{4}$$

where ν_1 and ν_2 are the Poisson's ratio of the particle and the surface (26). The Young's modulus of HOPG is 225 MPa (27). The Young's modulus of salbutamol was not determined; however, most crystalline drug compounds have a value in the range of 5–10 GPa (28–30). From this, the Young's modulus of both the micronized and SEDS™ salbutamol was taken as being 10 GPa. The value of ν for the HOPG and salbutamol was 0.3 (27,30). Using the values of E^* and R, the area of contact of the particle on the surface was calculated.

The contact area was then related to force data obtained for each of the particles by division of the force data by the surface area. The force distributions were then replotted using this corrected data.

To investigate the work of adhesion, one of two theories are typically used. The first is the Johnson-Kendall-Roberts (JKR) theory (31). This theory is based upon the consideration that surface forces act inside the contact region causing it to deform. These forces bring the two surfaces together to form a neck, thereby creating a contact area for a finite load. The pull-off force at this stage is as follows:

$$F_{ad} = \tfrac{3}{2}\pi\gamma R \tag{5}$$

where F_{ad} is the force of adhesion, and γ is the work of adhesion.

The second method is the Deryaguin–Muller–Toporov (32) theory. This theory also assumes that there are attractive forces that act to deform the sphere. However in this theory the attractive forces are acting outside the contact region. The pull-off force is given by the following:

$$F_{ad} = 2\pi\gamma R \tag{6}$$

To decide on which model to use, the parameter ϕ_0 is used as suggested by Tabor (33), where ϕ_0 is,

$$\phi_0 = \frac{[\Delta\gamma^2 R]}{[E^{*2} z_0^3]}^{1/3} \tag{7}$$

where z_0 is the equilibrium size of the atoms at contact. Tabor suggests that when ϕ_0 exceeds unity, the JKR theory is applicable, otherwise the Deryaguin–Muller–Toporov model is used. However the value a 0.3 has also been used (26). To define ϕ_0, the particle and the surface were assumed to come

into atomic contact, so the value of z_0 was taken to be the average atomic diameter of carbon (0.154 nm). The value of $\Delta\gamma$ was calculated from the surface free energy values determined using inverse gas chromatography (19). For both sets of data the value of ϕ_0 was found to be considerably above 0.3, indicating that the JKR model was more appropriate. By using the experimentally determined forces, the work of adhesion was determined, and this plotted as a frequency distribution.

RESULTS AND DISCUSSION

SEM Images

Examples of SEM images taken of the drug particles on the tips are shown in Fig. 2. These images show that particles had been successfully added on to the tips. In this example, the micronized salbutamol tip (a) showed that one particle expressing an irregular morphology with a diameter of approximately 10 μm had been adhered to the tip. The SEDS™ tip (b) also appeared to consist of one particle, again approximately 10 μm in diameter. The probe of the cantilever could not be observed on either tip, and thus it is unlikely that it would be able to contact the sample surface during subsequent force measurements.

Force Distance Data

Force data for the different particles and controls are displayed in Fig. 3. The regression coefficients of the data

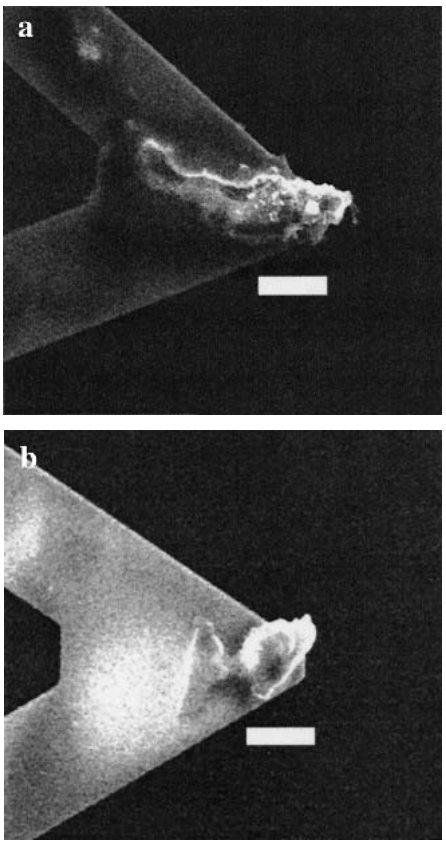

Fig. 2. Scanning electron microscopy images of tips with (a) micronized and (b) solution-enhanced dispersion by supercritical fluids salbutamol added onto tip apex (bar length 10 μm).

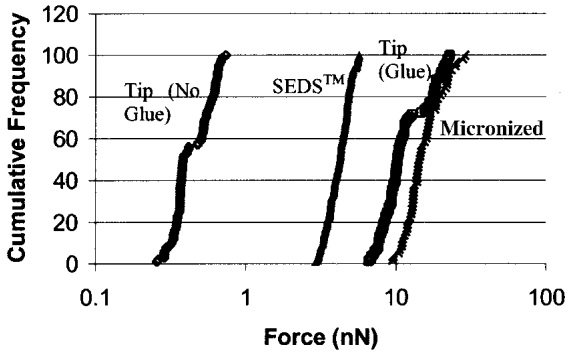

Fig. 3. Adhesion force data obtained for micronized salbutamol, solution-enhanced dispersion by supercritical fluids salbutamol, tip in no glue, and tip in glue.

indicated that a normal distribution is present for all the observed interactions, meaning that the distribution can be characterized by the geometric mean and standard deviation. It can be seen that there is a difference between the mean values of control data and the data for the particles. The mean force for the SEDS™ material is 4.2 nN (SD 0.8 nN), which is lower than that observed for the micronized material at 14.1 nN (SD 2.5 nN). The plasma-etched tip, however, had an average force of 0.4 nN (SD 0.1 nN) and the tip in glue had a corresponding average of 10.2 nN (SD 2.1 nN). The SD of the tip in glue does overlap slightly with the micronized particle. However, these data, combined with the images discussed later, indicate that it is unlikely that the cantilever tip is responsible for the interaction observed with the particle tips. It was also observed that the forces did not increase with the number of measurements taken, indicating that no triboelectric charging was occurring against the substrate.

Tip Imaging

The tip images of the particles and the control are displayed in Fig. 4. It is seen that the structure of the uncoated tip control image (c) is different to that obtained for the particle tips (a and b). This indicates that it is indeed the particles coming into contact with the surface during the force distance measurements and imaging, and not the tip. It can also be seen that the SEDS™ and micronized images differ both from each other, and also from their corresponding SEM images (Fig. 2).

The SEM data in Fig. 2 for the micronized salbutamol shows the presence of an elongated particle of irregular morphology. However, the tip image for this particle shows that that there were two asperities of sufficient height to be imaged by the grid. The larger asperity was approximately 1 μm wide, 0.5 μm long, and 0.35 μm high, whereas the smaller asperity was 0.6 μm wide, 0.35 μm long, and 0.15 μm high. The difference in height between the two was approximately 0.2 μm. Using the contact region distance (region b to c in Fig. 1), it was established that the smaller asperity would not be involved in the interaction.

The SEDS™ salbutamol also shows differences between the SEM and AFM data. The SEM image appeared to show a single particle approximately 10 μm long. However, the

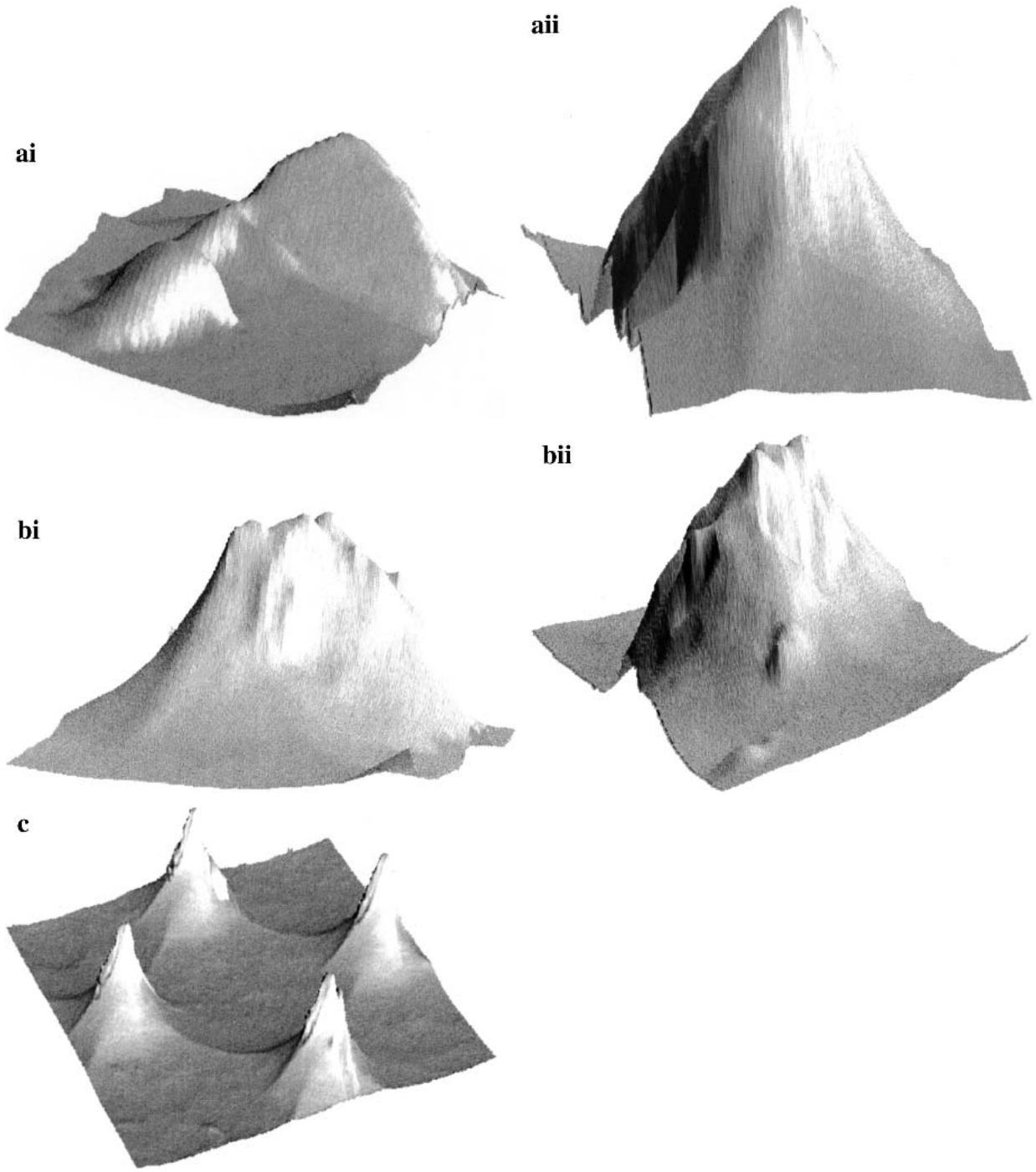

Fig. 4. Tip imaging images of (a) micronized (XY = 1.3 μm, Z = 500 nm), (ai) front of asperity, and (aii) back of asperity. (b) solution-enhanced dispersion by supercritical fluids salbutamol, (bi) front of asperity, and (bii) back of asperity (XY = 1.5 μm Z = 380 nm). (c) control tip (XY = 4 μm, Z = 400 nm).

AFM data shows the presence of an asperity that is approximately 1.5 μm wide, 1.2 μm long, and 0.45 μm high. This indicates that there is an area of the SEDS™ particle protruding from the surface, which is responsible for the observed interaction. If the SEM data had been used alone for contact area estimation, it would have lead to an overestimation of surface area. The AFM image is also different from the micronized salbutamol image in that the asperity appears to be more spherical in shape with a flatter edge at the top.

The AFM image of the control tip shows a series of peaks of a more regular cone like structure of approximate height 0.35μm and a width of 1.5μm. This is very different to the images seen with the particles on the end of the tip, and consistent with the expected structure for an AFM tip.

The tips were re-examined under the SEM after the experiment (images not shown). The particles were still present on the tips with no obvious change in the shape of the particle compared to the initial SEM images.

Processed Data

The surface area calculated for the micronized and SEDS™ salbutamol using the method discussed earlier are shown in Table I. The area of the micronized particle is 1.1×10^{-3} μm^2 and is smaller than that seen for the SEDS™ material of 1.4×10^{-3} μm^2.

The force data after correction for surface area are presented in Fig. 5. The average force per unit area of the micronized particle is 13.0 $mN\mu m^{-2}$ (SD 2.3 $mN\mu m^{-2}$). This is in comparison with the SEDS™ tip where the average force per unit area is 3.0 $mN\mu m^{-2}$ (SD 0.6 $mN\mu m^{-2}$).

The average work of adhesion of the particles calculated using the JKR theory described above is shown in Fig. 6. The average work of adhesion per unit area for the micronized particle was 19.0 mJm^{-2} (SD 3.4 mJm^{-2}). This is compared to an average value of 4.0 mJm^{-2} (SD 0.8 mJm^{-2}) for the SEDS™ tip.

The results obtained can be explained by considering the surface energy of the different particle systems. Inverse gas chromatography studies have shown that the SEDS™ salbutamol sulphate has a lower surface free energy than the micronized material (38.45 mJm^{-2} compared to 58.57 mJm^{-2}) and displays lower adhesion (17.0% w/w compared to 73.6% w/w; Refs. 34,35). Consistent with this work, we have shown that the SEDS™ material has a lower work of adhesion than the micronized. Because materials with a high surface free energy have high adhesive forces (36), the higher surface energy of the micronized material would account for the higher adhesion observed compared to the SEDS™ material. It is worth commenting that we have observed the work of adhesion of the micronized sample being approximately five times greater than that for the SEDS material, where as the surface energies from inverse gas chromatography are different by less than a factor of two. This is explained by considering Eq. (1). The work of adhesion is calculated by subtraction of the free energy of the interface between the substrate and particle from the combined sum of the separate free energies of the particle and substrate. This means that the differences between the two are dependent on the energy of the interface and not the surface energy of the particles alone, hence a direct quantitative comparison is not appropriate. In contrast, the relative adhesion measured using electric charge/adhesion for the SEDS and micronized salbutamol are in the approximate ratio 1 to 5 (34) as seen in the AFM data.

CONCLUSIONS

Determination of work of adhesion of pharmaceutical materials can be one of the critical factors in characterizing behavior during manufacture, processing and delivery. AFM has the potential to contribute to the techniques already used in such measurements through its ability to evaluate interactions between individual particles. We have demonstrated an important step to realizing this potential through the ability to normalize observed contact forces to the contact areas. In addition, we have shown how this can related to the work of adhesion. Individual particles of micronized and SEDS™ processed salbutamol were found to have initial adhesion forces of 14.1 nN (SD 2.5 nN) and 4.2 nN (SD 0.8 nN), respectively. After imaging of the surfaces of the particles, the potential contact surface areas were found to be 1.1×10^{-3} μm^2 for the micronized particle and $1.4 \times 10^{-3} \mu m^2$ for the SEDS™ particle. These values were then used to correct the adhesion force data for the influence of surface area. The forces per unit area were found to be 13 $mN\mu m^{-2}$ (SD 2.3 $mN\mu m^{-2}$) for the micronized particle and 3.0 $mN\mu m^{-2}$ (SD 0.6 $mN\mu m^{-2}$) for the SEDS™ particle. The forces were then related to the average work of adhesion using the JKR model. For the micronized material the work of adhesion was 19 mJm^{-2} (SD 3.4 mJm^{-2}). This is compared to an average value of 4.0 mJm^{-2} (SD 0.8 mJm^{-2}) for the SEDS™ material. These data are consistent with previous macroscopic inverse gas chromatography and electric charge adhesion studies (34,35).

In conclusion, using an AFM-based approach, it has been shown that it is possible to make direct quantitative comparison of particulate adhesion forces in a relevant model environment between particles produced using different manufacturing techniques, thereby overcoming one of the key limitations frequently noted for AFM force distance data acquisition on complex pharmaceutical materials.

Table I. Areas for Micronized Salbutamol and SEDS™ Salbutamol

Particle	Area of interaction (μm^2)
Micronized salbutamol	1.1×10^{-3}
Solution-enhanced dispersion by supercritical fluids salbutamol	1.4×10^{-3}

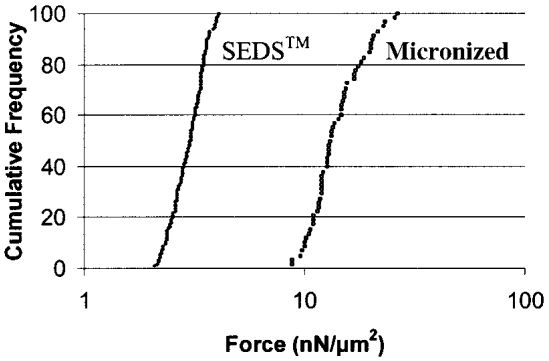

Fig. 5. Adhesion force data corrected for surface area of micronized and solution-enhanced dispersion by supercritical fluids salbutamol.

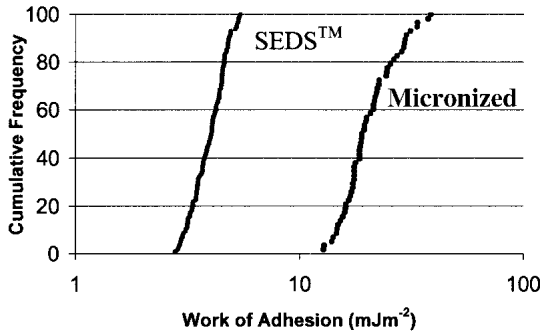

Fig. 6. Work of adhesion of micronized and solution-enhanced dispersion by supercritical fluids salbutamol.

ACKNOWLEDGMENTS

J.C.H. acknowledges the Biotechnology and Biologic Science Research Council and Bradford Particle Design Ltd for studentship funding.

REFERENCES

1. K. K. Lam and J. M. Newton. Effect of temperature on particulate solid adhesion to a substrate surface. *Powder Technol.* **73**: 117–125 (1992).
2. G. Binnig, C. F. Quate, and Ch. Gerber. Atomic force microscope. *Phys. Rev. Lett.* **56**:930–933 (1986).
3. W. A. Ducker and T. J. Senden. Measurement of forces in liquids using a force microscope. *Langmuir* **8**:1831–1836 (1992).
4. H. J. Butt. Measuring electrostatic, van der waals, and hydration forces in electrolyte solutions with an atomic force microscope. *Biophys. J.* **60**:1438–1444 (1991).
5. D. M. Schaefer, M. Carpenter, B. Gady, R. Reifenberger, L. P. Demejo, and D. S. Rimai. Surface roughness and its influence on particle adhesion using atomic force techniques. *J. Adhesion Sci. Technol.* **9**:1049–1062 (1995).
6. T. H. Ibrahim, T. R. Burk, F. M. Etzler, and R. D. Neuman. Direct adhesion measurements of pharmaceutical particles to gelatin capsule surfaces. *J. Adhesion Sci. Technol.* **14**:1225–1242 (2000).
7. M. D. Louey, P. Mulvaney, and P. J. Stewart. Characterisation of adhesional properties of lactose carriers using atomic force microscopy. *J. Pharm. Biomed. Anal.* **25**:559–567 (2001).
8. C. Vervaet and P. R. Byron. Drug-surfactant-propellant interactions in HFA formulations. *Int. J. Pharm.* **186**:13–30 (1999).
9. V. V. Yaminsky. Cavitation, polywater and hydrophobic attraction by bridging by flimsy shells. *Coll. Surf. A. Phys. Eng. Aspects* **129-130**:415–424 (1997).
10. F. Podczeck. *Particle-particle Adhesion in Pharmaceutical Powder Handling*, Imperial College Press, London, 1998, p. 29.
11. C. Neto and V. S. J. Craig. Colloid probe characterization: radius and roughness determination. *Langmuir* **17**:2097–2099 (2001).
12. P. York. Strategies for particle design using supercritical fluid technologies. *Pharma. Sci. Technol. Today* **2**:430–440 (1999).
13. J. H. Kim, T. E. Paxton, and D. L. Tomasko. Microencapsulation of naproxen using rapid expansion of supercritical solutions. *Biotechnol. Prog.* **12**:650–661 (1996).
14. P. Alessi, A. Cortesi, I. Kikic, N. R. Foster, S. J. Macnaughton, and I. Colombo. Particle production of steroid drugs using supercritical fluid processing. *Ind. Eng. Chem. Res.* **35**:4718–4726 (1996).
15. E. Reverchon, G. Della Porta, and P. Pallado. Supercritical antisolvent precipitation of salbutamol microparticles. *Powder Technol.* **114**:17–22 (2001).
16. D. J. Dixon, K. P. Johnston, and R. A. Bodmeier. Polymeric materials formed by precipitation with a compressed fluid antisolvent. *AIChE J.* **39**:127–139 (1993).
17. M. Hanna and P. York. *Method and apparatus for the formation of particles*, European Patent No. 9313642.2., 1993.
18. J. C. Feeley, P. York, B. S. Sumby, H. Dicks, and M. Hanna. In vitro assessment of salbutamol sulphate prepared by micronisation and a novel supercritical fluid technique. In *Drug Delivery to the Lungs IX*, The Aerosol Society, London, 1998 pp. 196–199.
19. J. C. Feeley, P. York, B. S. Sumby, and H. Dicks. Comparison of the surface properties of salbutamol sulphate prepared by micronization and a supercritical fluid technique. *J. Pharm. Pharmacol.* **50**:S54 (1998).
20. S. Bosewell, L. Esan, and P. Rogueda. Phase separation of non aqueous solid dispersions. In *Drug Delivery to the Lungs IX*, The Aerosol Society, London, 1998, p. 199.
21. J. L. Hutter and J. Bechhoefer. Calibration of atomic-force microscope tips. *Rev. Sci. Instrum.* **64**:1868–1873 (1993).
22. S. Kitching, P. M. Williams, C. J. Roberts, M. C. Davies, and S. J. B. Tendler. Quantifying surface topography and scanning probe image reconstruction. *J. Vac. Sci. Technol. B* **17**:273–279 (1999).
23. S. J. Villarrubia. Algorithms for scanned probe microscope image simulation, surface reconstruction, and tip estimation. *Natl. Inst. Stand. Technol.* **102**:435–454 (1997).
24. A. D. Zimon. *Adhesion of Dust and Powder*. Consultants Bureau, New York, 1982, p. 49.
25. D. Tabor. A simple theory of static and dynamic hardness. *Proc. Roy. Soc. A* **192**:247–274 (1948).
26. F. Podczeck, J. M. Newton, and M. B. James. The estimation of the true area of contact between microscopic particles and a flat surface in adhesion contact. *J. Appl. Phys.* **79**:1458–1463 (1996).
27. N. A. Burnham and R. J. Colton. Measuring the nanomechanical properties and surface forces of material using an atomic force microscope. *J. Vac. Sci. Technol. A* **7**:2906–2913 (1989).
28. W. C. Duncan-Hewitt and G. C. Weatherly. Evaluating the hardenss, Young's modulus and fracture toughness of some pharmaceutical crystals using microindentation techniques. *J. Mater. Sci. Lett.* **8**:1350–1352 (1989).
29. R. J. Roberts and R. C. Rowe. Brittle/ductile behaviour in pharmaceutical materials used in tableting. *Int. J. Pharm.* **36**:205–209 (1987).
30. R. J. Roberts, R. C. Rowe, and P. York. The relationship between Young's modulus of elasticity of organic solids and their molecular structure. *Powder Technol.* **65**:139–146 (1991).
31. K. L. Johnson, K. Kendall, and A. D. Roberts. Surface energy and the contact of elastic solids. *Proc. R. Soc. Lond. A* **324**:301–313 (1971).
32. B. V. Derjaguin and V. M. Muller. and Yu. P. Toporov. Effect of contact deformations on the adhesion of particles. *J. Colloid Interface Sci.* **53**:314–326 (1975).
33. D. Tabor. Surface forces and surface interactions. *J. Colloid Interface Sci.* **58**:2–13 (1977).
34. J. C. Feeley, B. Y. Shekunov, A. H. L. Chow, and P. York. Surface and aerodynamic characteristics of particles for inhalation produced using supercritical fluid technology. *Proc. Millennium World Congress Pharm. Sci.* (2000)
35. I. M. Grimsey, J. C. Feeley, and P. York. Analysis of the surface energy of pharmaceutical powder by inverse gas chromatography. *J. Pharm. Sci.* **91**:571–583 (2002).
36. X. M. Zeng, G. P. Martin, and C. Marriott. *Particulate Interactions in Dry Powder Formulations for Inhalation*, Taylor & Francis Inc, London, 2001, p. 21